JOURNAL OF Applied Polymer SCIENCE

Magnetite/Polypyrrole Hybrid Nanocomposites as a Promising Magnetic Resonance Imaging Contrast Material

Kleber G. B. Alves,[1] Cesar A. S. Andrade,[2] Sergio L. Campello,[3] Ricardo E. de Souza,[3,4] Celso P. de Melo[3,4]

[1]Departamento de Engenharia Mecânica, Universidade Federal de Pernambuco, Recife 50670-901, Pernambuco, Brazil
[2]Departamento de Bioquímica, Universidade Federal de Pernambuco, Recife 50670-901, Pernambuco, Brazil
[3]Pós-Graduação em Ciência de Materiais, Universidade Federal de Pernambuco, Recife 50670-901, Pernambuco, Brazil
[4]Departamento de Física, Universidade Federal de Pernambuco, Recife 50670-901, Pernambuco, Brazil
Correspondence to: C. P. de Melo (E-mail: celso@df.ufpe.br)

ABSTRACT: We have prepared magnetite nanoparticles (Fe_3O_4_NPs) almost spherical in shape with average particle size of 10 nm and successfully encapsulated them in an envelope of polypyrrole (PPY) chains via an emulsion polymerization route using sodium dodecyl sulfate as surfactant. The resulting PPY-coated Fe_3O_4_NPs (Fe_3O_4_NPs/PPY) suspensions were stable with particles exhibiting a triangular prismatic morphology and an average diameter below 100 nm. In fact, all colloidal solutions were stable in aqueous media with typical ζ-surface potential values of -33.9 mV (Fe_3O_4_NPs) and -20.0 mV (Fe_3O_4_NPs/PPY). Although X-ray diffraction studies revealed the presence of a magnetic phase Fe_3O_4, the identified diffraction peaks are consistent with the presence of a spinel structure of magnetite. A ferromagnetic behavior, such as lower coercive force ($H_c = 0.065$ T), was observed for all magnetic nanoparticles examined. The ^{1}H NMR relaxation times T_1 and T_2 of selected Fe_3O_4_NPs/PPY samples were also measured and their relaxivities r_1 (1.1 s^{-1} mM^{-1}) and r_2 (61.9 s^{-1} mM^{-1}) compare favorably to those of contrast agents commercially used in human examinations. We suggest that the present results indicate that these hybrid nanocomposites are promising materials for the development of a platform of specialized contrast agents for ^{1}H Magnetic Resonance Imaging. © 2012 Wiley Periodicals, Inc. J. Appl. Polym. Sci. 000: 000–000, 2012

KEYWORDS: nanocomposites; surfactants; conducting polymers; colloids

Received 12 June 2012; accepted 16 August 2012; published online
DOI: 10.1002/app.38481

INTRODUCTION

Polypyrrole (PPY), one of the best-studied conducting polymers, has received large attention as active component of nanocomposites owing to the high environmental stability of its conducting oxidized form. Although biological and health applications of this polymer include its use for the immobilization of enzymes, antibodies, and nucleic acids,[1] there has been an increased interest in exploiting the excellent *in vivo* biocompatibility of this material.[2–4] At the same time, Fe_3O_4 particles, named magnetite, have been widely studied because of their large range of possible applications in the preparation of ferrofluids and catalytic materials, and as active elements in biological assays and chemical sensors.[5,6] However, magnetite *micro*particles do not seem appropriate for use in magnetic resonance imaging (MRI) owing to the lack of sufficient contrast-to-noise ratio associated to the limited signal intensity. Things are different for iron oxide *nano*particles as substantial changes in the magnetic properties occur in this domain size as consequence of quantum confinement effects related to their large surface to volume area. In fact, iron oxide nanoparticles have been shown to play an important role as MRI contrast agents in many *in vivo* applications owing to the capability of allowing a better differentiation between healthy and pathological tissues.[7] As the parameters T_1 (spin–lattice or longitudinal relaxation time) and T_2 (spin–spin or transverse relaxation time) may differ from one tissue to the next, they can be used as a source of contrast in MRI images. The enhanced image definition obtained with the use of contrast agents of different T_2/T_1 ratios enables particular tissues to be visualized by increasing or decreasing the signal level of the particular area of interest relative to that of its surroundings. Contrast agents increase both longitudinal T_1^{-1} and transverse T_2^{-1} relaxation rates; those that raise the signal level of the target site relative to that of its surroundings are termed positive contrast agents, whereas those lowering the signal level relative to their immediate vicinity are termed negative contrast agents.[8] Although the former causes a reduction in the T_1 relaxation time, resulting in brighter images, negative

contrast agents (such as the superparamagnetic iron oxides) enhance the local field inhomogeneity that favor spin–spin relaxation effects (leading to shorter T_1 and T_2 relaxation times) and appear predominantly dark on MRI. Manganese, gadolinium complexes, or iron is widely used as positive contrast agent for routine MRI, whereas magnetite nanoparticles (ultrasmall particles iron oxide nanoparticles [USPION] and small particles iron oxide nanoparticles [SPION]) belong to the second category of negative agents for MRI.[9]

Use of a contrast agent X at a concentration [X] affects each relaxation rate $R_i = T_i^{-1}$ through the relationship

$$R_i = \left(T_i^{-1}\right) = (T_i)_0^{-1} + r_i[X] \quad (1)$$

where $i = 1,2$, $(R_i)_0 = (T_i)_0^{-1}$ is the corresponding relaxation rate in the absence of the contrast agent and r_i its relaxivity.[10,11] For proton-based MRI, the number, relative position, and residence time of water molecules in the innermost internal structure of the particles are determining factors of the corresponding relaxivity, a fact of special relevance to the present study. Hence, control of the relaxivity value can be achieved by varying different factors, such as the nature, overall size, and internal structure of the particles of the contrast agent.[11] For instance, the transverse r_2 of superparamagnetic nanoparticles is far greater than their longitudinal r_1, a fact that explains the reason why they are used mainly as negative contrast agents for improved visualization of organs such as the liver, spleen, and brain.[9]

Recently, use of surfactants for the preparation of hybrid microcomposites of PPY and Fe_3O_4 by wet chemistry methods has been reported,[12] and the electric and magnetic properties of these (iron oxide)/(conducting polymer) composites have been extensively investigated.[13–16] Extensive research has been focused on the synthesis of polymeric nanocomposites and on the evaluation of their potential applications as MRI contrast agents.[17–19]

One should also note that Wuang and coworkers have synthesized Fe_3O_4 nanoparticles encapsulated in a PPY envelope via an emulsion polymerization technique that used polyvinyl alcohol as a surfactant.[1] The resulting nanocomposites not only exhibited typical superparamagnetic characteristics but were also cytocompatible and have been used to identify the presence of human breast cancer cells, after surface functionalization with folic acid (an efficient cancer cell targeting agent). Hence, the use of (conducting polymer)/Fe_3O_4_NPs nanocomposites opens up not only the possibility of more specialized target imaging, but also brings a little closer the futuristic idea of "theranostic" particles,[11] that is, contrast agents that could play the additional role of drug delivers at specially localized sites.

In the present study, we initially report the method of synthesis of Fe_3O_4_NPs/PPY composites based on the chemical polymerization of pyrrole in aqueous media in presence of Fe_3O_4_NPs and sodium dodecyl sulfate (SDS), an anionic surfactant. Then, we first discuss the characterization of these hybrid nanocomposites by structural analyses (X-ray diffraction [XRD], dynamic light scattering (DLS), ζ-potential measurements, and transmission electron microscopy [TEM]), the determination of magnetic properties, and use of spectroscopic (Fourier transform infrared [FTIR] and nuclear magnetic resonance) techniques. Finally, we present a first evaluation of the potential applicability of the Fe_3O_4_NPs/PPY hybrid composites as MRI contrast agents, a possibility that, to the best of our knowledge, has not been yet discussed in the literature.

MATERIALS AND METHODS

Chemicals

Pyrrole and high-purity SDS were purchased from Sigma-Aldrich (USA). Although pyrrole was previously distilled under vacuum and subsequently stored in a dark recipient under refrigeration before use, SDS and the other analytical-grade reagents needed for the preparation of the magnetic particles ($FeSO_4{\cdot}7H_2O$ [Reagen, Brazil], $FeCl_3{\cdot}6H_2O$ [Synth, Brazil] and NH_4OH [Quimex, Brazil]) were used as received.

Synthesis of Fe_3O_4_NPs and Fe_3O_4_NPs/PPY

Initially, magnetite nanoparticles were obtained by chemical coprecipitation method, a technique that we have previously used for obtaining Fe_3O_4 microparticles.[12] First, we prepared a 1*M* $FeCl_3{\cdot}6H_2O$ and 1.5*M* $FeSO_4{\cdot}7H_2O$ solution using ultrapure water obtained from a Nanopure system (Barnstead, USA). A volume equal to 50 mL of this solution was then transferred to a three-necked round-bottomed flask and maintained under intense stirring at room temperature for 10 min and then 50 mL of NH_4OH (50%) was quickly added to the bottom flask until the liquid turned blackish. The system was then stirred for an additional period of 2 h. The precipitate separated by magnetic decantation was washed with deionized water several times, and twice with ethanol, and finally evaporated to dryness to yield the final magnetic nanoparticle iron oxide powder.

After this, Fe_3O_4_NPs/PPY composites were prepared via *in situ* chemical polymerization in an aqueous solution containing Fe_3O_4_NPs and SDS. The polymerization was carried out in a 100-mL two-necked round-bottomed flask equipped with a mechanical stirrer. Typically, 20 mL of deionized water, 12 m*M* of SDS and 21 m*M* of Fe_3O_4_NPs were initially placed in the flask and stirred at room temperature for 20 min. Then, 250 m*M* of pyrrole was added and the mixture was stirred for 1 h after which the polymerization was started by the addition of 400 μL of a 1*M* aqueous solution of $FeCl_3$. Finally, the system was kept under stirring for 24 h.

For a better understanding of the properties of the above samples, we have also prepared pure PPY colloidal solutions. The corresponding samples were obtained by following the same procedure described for the case of the preparation of Fe_3O_4_NPs/PPY but in the absence of Fe_3O_4_NPs. The corresponding DRX and FTIR were used for a comparative analysis to those of the other samples.

Characterization

A ZS90 NanoZetasizer instrument (Malvern, United Kingdom) was used to determine the properties of the colloidal samples dispersed in water at a temperature of 25°C; particle size distribution was estimated by the DLS of a $\lambda = 633$ nm laser at a 90° scattering angle, whereas the electrophoretic method was used for the determination of the ζ-potential of the colloidal suspension. All reported results correspond to the average of three independent measurements.

The size and shape distributions of the resulting nanoparticles were assessed from TEM micrographs obtained using carbon coated 400 mesh copper grids at an accelerating voltage of 80 kV in a Tecnai G^2 Spirit microscope (FEI, USA) equipped with a CCD camera. The corresponding size distribution of the particles was estimated by use of ImageJ software.[20] FTIR spectra of the KBr compressed thin disks of the desired samples were recorded on an ABB FTLA 2000 spectrometer (Bomem, Canada), under transmission mode at the 400–1800 cm^{-1} region, with a resolution of 4 cm^{-1}.

XRD diagrams were obtained with a Siemens D5000 (Siemens, Germany) using CuKα radiation. Magnetic characterization of the samples was carried out at room temperature at Prof. J. H. de Araújo's laboratory at the Universidade Federal do Rio Grande do Norte (Brazil), by use of a homemade vibrating sample magnetometer operating with applied magnetic fields up to 1.17 T.[21] We have assessed the possibility of using this material as a contrast agent for MRI by implementing nuclear magnetic resonance (NMR) measurements where the relevant data were acquired by a Unity Inova NMR spectrometer (Varian, USA) at a fixed value (B_0 = 2.04 T) of the magnetic field. The spin–lattice T_1 and spin–spin T_2 NMR relaxation times were obtained from inversion-recovery and Carl–Purcell–Meiboom–Gill pulse sequence,[22] respectively, as a function of iron concentration for the Fe_3O_4_NPs and Fe_3O_4_NPs/PPY composites in aqueous solutions.

RESULTS AND DISCUSSION

TEM and DLS

In Figure 1 we show the morphology of both pure Fe_3O_4_NPs and Fe_3O_4_NPs/PPY composites, as revealed by TEM. Samples of Fe_3O_4_NPs were nearly uniformly spherical, with average particle size 10.2 ± 3.9 nm [Figure 1(a)]; the presence of some aggregates, which probably result from mutual magneto–dipole interactions, could be identified.[23] On the other hand, the TEM images of PPY-coated Fe_3O_4_NPs [Figure 1(b)] reveal that they present a triangular morphology, with easily recognized independent Fe_3O_4_NPs cores [Figure 1(c)], and size of particle seem to be mostly below 100 nm, an average size that should be compared with those of commercial SPION contrast agents: ENDOREN™ (156 nm) and RESOVIST™ (75 nm).[24] Surfactant self-assemblies have been employed as soft templates to control the size and shape of nanoparticles with particular morphologies in solution because of their hydrophilic and lipophilic properties in what it is called a wet chemical method.[25] Surfactant micellar solutions have been used to synthesized nanostructures with morphology of triangles,[25] rings, and hexagons.[26] Recently, conducting polymer samples in various forms of hierarchic nanostructures of different morphology (rhomboids, corals, dish like, globules, and nanowires shape) have been successfully synthesized and, by varying the synthesis parameters, it is possible to obtain various nanostructures and materials with different properties.[27]

Sui et al.[28] have already discussed the use of surfactant micelles and microemulsions as nanoreactors, in an example of a shape-control method, when nanocomposites of polyaniline/TiO_2 with triangular morphology were successfully synthesized in reverse micelles with sodium *bis*(2-ethylhexyl) sulfosuccinate as the surfactant.

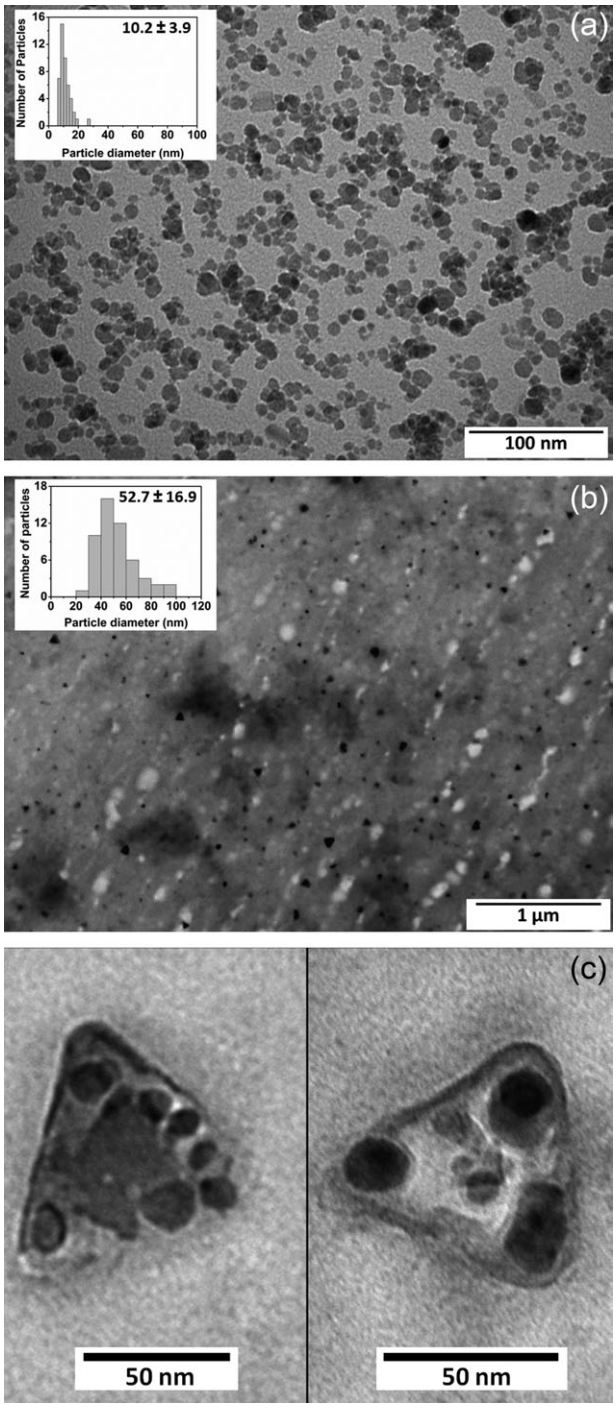

Figure 1. TEM images of pure Fe_3O_4_NPs (a), Fe_3O_4_NPs/PPY nanocomposites (b) and high-magnification TEM images of Fe_3O_4_NPs/PPY nanocomposites (c). Insets in (a) and (b) show particle size distribution of the samples obtained from the respective TEM images.

The particle size distribution for the colloids as characterized by DLS is shown in Figure 2. Although for the pure Fe_3O_4_NPs the average particle diameter was found to be 9.7 ± 3.1 nm, with a relatively narrow distribution, a value of be 63.1 ± 23.1 nm was found in the case of the Fe_3O_4_NPs/PPY nanocomposites.

Applied Polymer SCIENCE

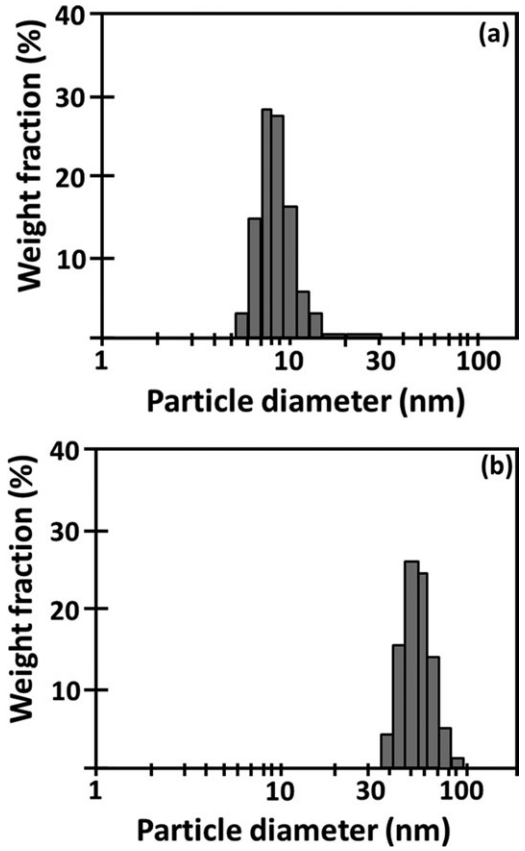

Figure 2. Particle size distribution of pure Fe_3O_4_NPs (a) and Fe_3O_4_NPs/PPY (b) colloidal suspensions characterized by DLS.

ζ-Potential Measurements

The ζ-values of the particles present in the aqueous colloidal solutions were determined to be negative and the corresponding average values obtained were −33.9 mV (for Fe_3O_4_NPs) and −20.0 mV (Fe_3O_4_NPs/PPY). The ζ-values of the Fe_3O_4_NPs/PPY colloidal solutions decreased with increasing pH values (Figure 3). In addition, the Fe_3O_4_NPs/PPY composites presented a good stability with no evidence of precipitates or formation of agglomerates at the pH range from 3 to 11. The

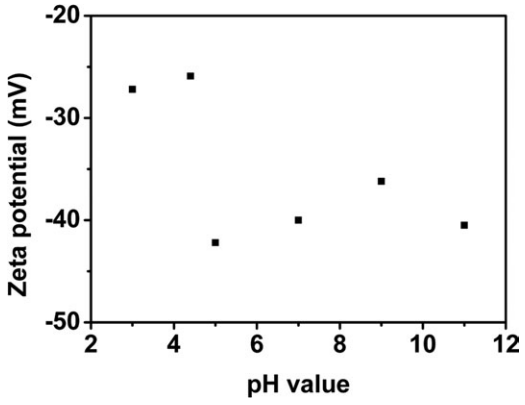

Figure 3. ζ-Potentials of Fe_3O_4_NPs/PPY colloidal dispersions at different pH values.

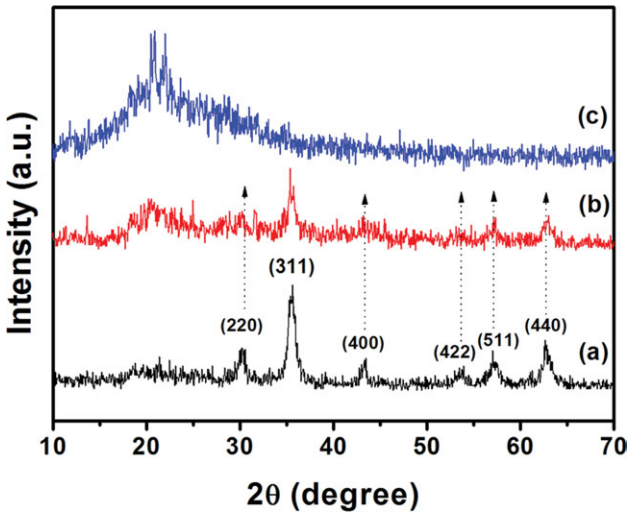

Figure 4. Diffractogram of Fe_3O_4_NPs (a), Fe_3O_4_NPs/PPY composites (b), and pure PPY (c). [Color figure can be viewed in the online issue, which is available at wileyonlinelibrary.com.]

importance of preparing these hybrid nanoparticles accordingly to a previously stipulated synthesis becomes evident if one recalls that in iron-oxide materials the transverse relaxation rate T_2^{-1} of protons shows a broad maximum for particles with size ~ 100 nm[29] and also that the average diameter of these nanoparticles plays a crucial role in reducing their toxicity and in improving their tissular diffusion.[30] In fact, polymers have been used to coat iron oxide particles as a manner to inhibit the *in vivo* adsorption of biological elements, especially proteins, which is the first step for activation of the mononuclear phagocyte system.[31]

X-ray Diffraction

The XRD patterns of pure PPY sample, Fe_3O_4_NPs, and Fe_3O_4_NPs/PPY nanocomposites are shown in Figure 4. The main peak characteristics of Fe_3O_4_NPs were found at 2θ = 30.2° (d = 0.297 nm), 35.6° (d = 0.253 nm), 43.1° (d = 0.209 nm), 53.6° (d = 0.171 nm), 57.3° (d = 0.162 nm), and 62.8° (d = 0.147nm), which correspond to the (220), (311), (400), (422), (511), and (440) Bragg reflections, respectively; this set of results allows the identification of the Fe_3O_4_NPs as disposed in a cubic spinel structure.[32] The average diameter of the Fe_3O_4_NPs as measured in Angstroms can be found according to Scherrer's equation[33]: choosing the reflecting peak at 2θ = 35.6°, the estimated average size of the Fe_3O_4_NPs is 10 nm, a value consistent with the TEM results. Figure 4(c) shows the presence of the amorphous phase characteristic of pure PPY samples as the features visualized in the 15.8–27.2° 2θ interval, which is typical of a doped PPY structure.[34]

FTIR Spectroscopy

FTIR measurements of the nanocomposites show the presence of peaks at 1546 and 1467 cm^{-1}, corresponding to the C—C and C—N pyrrole ring stretching vibration, respectively[35] (Figure 5). The peak near 1216 cm^{-1} corresponds to the breathing vibration of the pyrrole ring and the peaks at 1046 and 965 cm^{-1} can be assigned to the =C—H in-plane and out-of-plane vibrations, respectively[36]; the peaks at 921 and 794 cm^{-1}

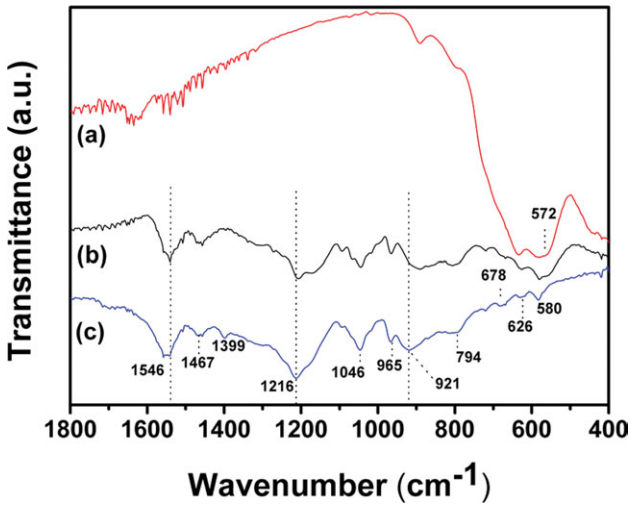

Figure 5. FTIR spectra of Fe_3O_4_NPs (a), Fe_3O_4_NPs/PPY composites (b), and pure PPY (c) [Color figure can be viewed in the online issue, which is available at wileyonlinelibrary.com.]

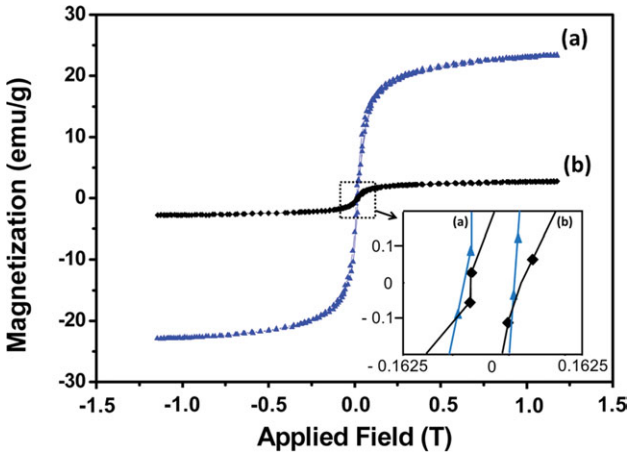

Figure 6. Magnetization curves at room temperature of Fe_3O_4_NPs (a), Fe_3O_4_NPs/PPY composites (b). Inset: Blow-up of these curves for the zero-field region. [Color figure can be viewed in the online issue, which is available at wileyonlinelibrary.com.]

correspond to the band of C—H out-of-plane deformation vibrations of the pyrrole ring, and the peak at 678 cm^{-1} can be attributed to the C—C out-of-plane ring deformation. Finally, the band at 626 cm^{-1} corresponds to a sulfate group band (attributed to SDS),[37] whereas the peak at 576 cm^{-1} is attributed to the Fe—O bond vibration in the Fe_3O_4 group.[38] The observed shift of the 1546, 1216, and 921 cm^{-1} peaks toward lower wavenumbers is suggestive of the existence of hydrogen bonds between the nitrogen atoms in the PPY chains and the magnetic nanoparticles in the Fe_3O_4_NPs/PPY hybrid nanocomposite. Other authors reported similar results for Fe_3O_4/PPY nanoparticles with core-shell structure.[23]

Magnetic Characteristics

A ferromagnetic behavior is observed in the magnetization curves of the samples shown in Figure 6. Owing to their size (diameter, <30 nm), the individual Fe_3O_4_NPs were expected to be superparamagnetic at room temperature[39]; instead, a small coercivity of 0.065 T was detected (inset of Figure 6). This can be attributed to a residual magnetic interaction between adjacent nanoparticles.[40] True superparamagnetic materials do not retain magnetic behavior after the removal of the applied magnetic field,[41] a convenient property in terms of preventing the formation of aggregates. The values of saturation magnetization (M_s) were 2.7 and 23.5 emu g^{-1} for the Fe_3O_4_NPs/PPY and Fe_3O_4_NPs, respectively (Figure 6). The M_s values of the nanocomposites are lower than the corresponding values of the Fe_3O_4_NPs, probably because the former is embedded into a nonmagnetic polymer matrix.[42,43] In addition, the obtained Fe_3O_4_NPs/PPY nanocomposite and Fe_3O_4_NPs presented lower M_s values compared to bulk magnetite (84 emu g^{-1}).[44]

NMR measurements of the Fe_3O_4_NPs and Fe_3O_4_NPs/PPY nanocomposites are shown in Figure 7. All measurements were carried out at 22°C. Accordingly to eq. (1), the r_1 and r_2 relaxivities were calculated from the angular coefficient of the relaxation rates as function of iron concentration.[11,45] From the data shown in Figure 7(a, b), we obtained $r_1 = 1.1$ s^{-1} mM^{-1} and $r_2 = 61.9$ s^{-1} mM^{-1} for the Fe_3O_4_NPs/PPY nanocomposite. As for the pure Fe_3O_4_NPs sample, the corresponding results are $r_1 = 8.76$ s^{-1} mM^{-1} (inset of Fig. 7(a)) and $r_2 = 68.5$ s^{-1} mM^{-1} (inset of Fig. 7(b)).

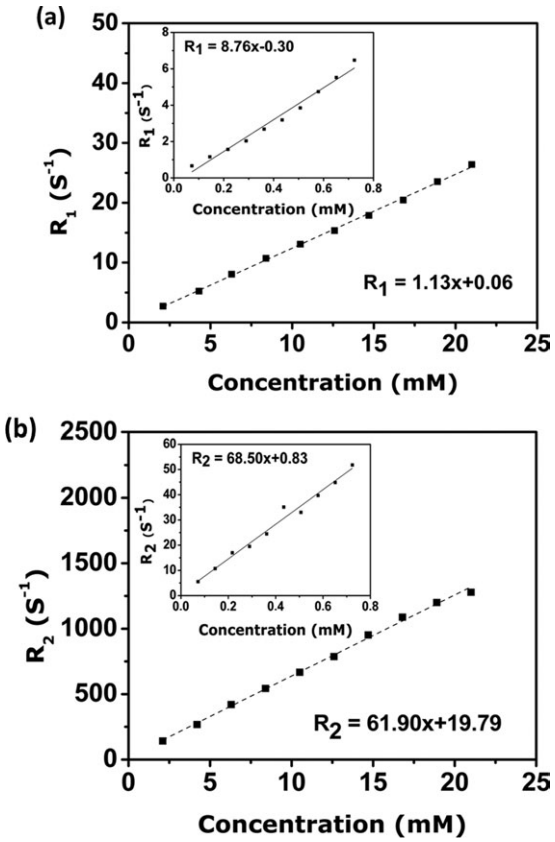

Figure 7. Plot of the relaxation rates r_1 (a) and r_2 (b) as a function of iron concentration for the Fe_3O_4_NPs/PPY composites. Inset: r_1 (a) and r_2 (b) as a function of iron concentration in the case of Fe_3O_4_NPs.

Our results are in general agreement with those values obtained from a theory describing water proton relaxation via magnetic interactions with nanoparticles.[46] These values could be compared with the r_2 relaxivities of commercial contrast agents commonly used in human MRI examinations, such as USPION (or MION-46, approximately 19.6 s^{-1} mM^{-1}),[47] Clariscan (or NC100150, 36.4 s^{-1} mM^{-1})[48] and Sinerem (or AMI-227, 53.1 s^{-1} mM^{-1}).[49] In fact, the Fe_3O_4_NPs/PPY nanocomposites present a core diameter smaller than 20 nm and total diameter ranging from 40 to 100 nm, resulting in an association distance between the enclosed Fe_3O_4_NPs and the water molecules that is greater than the equivalent distance for the case of pure Fe_3O_4_NPs. (note, however, that the r_2 value remains high for Fe_3O_4_NPs/PPY nanocomposite). We believe that these results are suggestive of the possibility of synthesizing high r_2 values PPY-coated Fe_3O_4_NPs with a total diameter greater than $\sim$ 100 nm. It is important to consider that a beneficial characteristic of an iron-based MRI contrast agent is to have a coated shell as thick as possible to avoid the poisoning of the patient by eventual side reactions with iron. Considering the magnetic behavior and the biocompatibility of Fe_3O_4 and PPY, these Fe_3O_4_NPs/PPY nanocomposites appear as promising candidates for the development of negative MRI contrast agents and related biomedical applications.

CONCLUSIONS

In this study, we have discussed the synthesis of pure Fe_3O_4_NPs by a chemical coprecipitation method and reported the preparation of conducting Fe_3O_4_NPs/PPY nanocomposites via chemical polymerization of pyrrole in the presence of Fe_3O_4_NPs and SDS. TEM revealed that the Fe_3O_4_NPs with small size (average size, 10.2 $\pm$ 3.9 nm), and that the resulting Fe_3O_4_NPs/PPY nanocomposites with triangle-shaped morphology and have average particle diameter below 100 nm. A ferromagnetic behavior was observed for all magnetic nanoparticles examined such as lower coercive force and the saturated magnetization is influenced by the polymeric coating of the Fe_3O_4_NPs. Our relaxivity measurements reveal that although both pure Fe_3O_4_NPs and Fe_3O_4_NPs/PPY composites have high transverse relaxivities r_2, the r_1 values are substantially affected by the presence of the PPY coating; hence, at least in principle, one has the possibility of controlling the T_2/T_1 ratio of the hybrid magnetite/PPY nanocomposites over a larger range of values. The magnetic properties and ^{1}H NMR relaxation times of these hybrid nanocomposites suggest that they are suitable for use as negative contrast agents for MRI of varying contrast ratios.

We have recently initiated studies related to the application of these materials to obtain images of biological tissues.

ACKNOWLEDGMENTS

The authors are grateful for the partial support from the Brazilian National Council for Scientific and Technological Development (CNPq) and PETROBRAS. K.G.B.A. and S.L.C. thank CAPES for graduate scholarships. The authors thank Dr. A. H. Shinohara (UFPE) and Dr. J. H. de Araújo (UFRN) for their generous assistance with FTIR and VSM measurements, respectively.

REFERENCES

1. Neoh, K. G.; Wuang, S. C.; Kang, E. T.; Pack, D. W.; Leckband, D. E. *J. Mater. Chem.* **2007,** *17*, 3354.
2. Ateh, D. D.; Vadgama, P.; Navsaria, H. A. *Tissue Eng.* **2006,** *12*, 645.
3. Sanghvi, A. B.; Miller, K. P. H.; Belcher, A. M.; Schmidt, C. E. *Nat. Mater.* **2005,** *4*, 496.
4. Fonner, J. M.; Forciniti, L.; Nguyen, H.; Byrne, J. D.; Kou, Y. F.; Syeda-Nawaz, J.; Schmidt, C. E. *Biomed. Mater.* **2008,** *3*, 034124.
5. Pankhurst, Q. A.; Thanh, N. K. T.; Jones, S. K.; Dobson, J. *J. Phys. D Appl. Phys.* **2009,** *42*, 224001.
6. Geus, J. W. *Appl. Catal.* **1986,** *25*, 313.
7. Gupta, A. K.; Gupta, M. *Biomaterials* **2005,** *26*, 3995.
8. Cunningham, C. H.; Arai, T.; Yang, P. C.; McConnell, M. V.; Pauly, J. M.; Conolly, S. M. *Magn. Reson. Med.* **2005,** *53*, 999.
9. Gossuin, Y.; Gillis, P.; Hocq, A.; Vuong, Q. L.; Roch, A. *Wiley Interdiscip. Rev. Nanomed. Nanobiotechnol.* **2009,** *1*, 299.
10. Pereira, G. A.; Norek, M.; Peters, J. A.; Ananias, D.; Rocha, J.; Geraldes, C. F. G. C. *Dalton Trans.* **2008,** *17*, 2241.
11. Que, E. L.; Chang, C. *J. Chem. Soc. Rev.* **2010,** *39*, 51.
12. de Oliveira, H. P.; Andrade, C. A. S.; de Melo, C. P. *J. Colloid Int. Sci.* **2008,** *319*, 441.
13. Qiu, G. H.; Wang, Q.; Nie, M. *Macromol. Mater. Eng.* **2006,** *291*, 68.
14. Khan, A.; Aldwayyan, A. S.; Alhoshan, M.; Alsalhi, M. *Polym. Int.* **2010,** *59*, 1690.
15. Zhu, H.; Guo, H. F.; Lin, H. Y.; Zhang, J. Q. *Mater. Lett.* **2008,** *62*, 2196.
16. Qiu, G. H.; Wang, Q.; Nie, M. *J. Appl. Polym. Sci.* **2006,** *102*, 2107.
17. Gatjens, J.; Liu, Z.; Lammers, T.; Ehling, J.; Fokong, S.; Bornemann, J.; Kiessling, F. *Biomaterials* **2011,** *32*, 6155.
18. Yu, J. H.; Zhang, W. L.; Li, N.; Huang, J.; Wang, D. X.; Li, Y. P.; Liu, S. Y. *J. Appl. Polym. Sci.* **2010,** 118, 1805.
19. Hua, M.; Yang, H.; Tsai, R.; Wei, K.; Chen, P.; Liu, H.; Hua, M.; Yang, H.; Tsai, R.; Wei, K.; Chen, P.; Liu, H. US Pat./US2011/0104077-A1, **2011.**
20. Ghosh, M.; Song, X. Y.; Mouneimne, G.; Sidani, M.; Lawrence, D. S.; Condeelis, J. S. *Science* **2004,** *304*, 743.
21. Borges, F. M. M.; Melo, D. M. A.; Camara, M. S. A.; Martinelli, A. E.; Soares, J. M.; de Araujo, J. H.; Cabral, F. A. O. *J. Magn. Magn. Mater.* **2006,** *302*, 273.
22. Fukushima, E.; Roeder, S. B. W. Experimental Pulse NMR: A Nuts and Bolts Approach; Addison-Wesley Pub. Co., Advanced Book Program: Reading, Massachusetts, **1981.**
23. Deng, J. G.; Peng, Y. X.; He, C. L.; Long, X. P.; Li, P.; Chan, A. S. C. *Polym. Int.* **2003,** *52*, 1182.
24. Morales, M. P.; Bomati-Miguel, O.; de Alejo, R. P.; Ruiz-Cabello, J.; Veintemillas-Verdaguer, S.; O'Grady, K. *J. Magn. Magn. Mater.* **2003,** *266*, 102.

25. Pinna, N.; Weiss, K.; Sack-Kongehl, H.; Vogel, W.; Urban, J.; Pileni, M. P. *Langmuir* **2001,** *17*, 7982.
26. Maillard, M.; Motte, L.; Ngo, A. T.; Pileni, M. P. *J. Phys. Chem. B* **2000,** *104*, 11871.
27. Shishov, M. A.; Moshnikov, V. A.; Sapurina, I. Y. *Glass Phys. Chem.* **2011,** *37*, 106.
28. Sui, X. M.; Chu, Y.; Xing, S. X.; Yu, M.; Liu, C. Z. *Colloid Surf. A* **2004,** *251*, 103.
29. Chen, D. X.; Sun, N.; Huang, Z. J.; Cheng, C. M.; Xu, H.; Gu, H. C. *J. Magn. Magn. Mater.* **2010,** *322*, 548.
30. Portet, D.; Denizot, B.; Rump, E.; Lejeune, J. J.; Jallet, P. *J. Colloid Interface Sci.* **2001,** *238*, 37.
31. Vanbeers, B.; Pringot, J.; Gallez, B. *J. Radiol.* **1995,** *76*, 991.
32. JCPDS-International Centre for Diffraction Data; International Centre for Diffraction Data: Newtown Square, Pennsylvania, **1992.**
33. Klug, H. P.; Alexander, L. E. X-ray Diffraction Procedures for Polycrystalline and Amorphous Materials, 2nd ed.; Wiley: New York, **1974.**
34. Ong, C. K.; Ray, S.; Cooney, R. P.; Edmonds, N. R.; Easteal, A. J. *J. Appl. Polym. Sci.* **2008,** *110*, 632.
35. Hosseini, M. G.; Bagheri, R.; Najjar, R. *J. Appl. Polym. Sci.* **2010,** *121*, 3166.
36. Selvaraj, M.; Palraj, S.; Maruthan, K.; Rajagopal, G.; Venkatachari, G. *J. Appl. Polym. Sci.* **2010,** *116*, 1524.
37. Omastova, M.; Trchova, M.; Kovarova, J.; Stejskal, J. *Synth. Met.* **2003,** *138*, 447.
38. Hong, R. Y.; Feng, B.; Cai, X.; Liu, G.; Li, H. Z.; Ding, J.; Zheng, Y.; Wei, D. G. *J. Appl. Polym. Sci.* **2009,** *112*, 89.
39. Ge, J. P.; Hu, Y. X.; Biasini, M.; Beyermann, W. P.; Yin, Y. D. *Angew. Chem. Int. Ed.* **2007,** *46*, 4342.
40. Hutten, A.; Sudfeld, D.; Ennen, I.; Reiss, G.; Wojczykowski, K.; Jutzi, P. *J. Magn. Magn. Mater.* **2005,** *293*, 93.
41. Chen, F.; Gao, Q.; Hong, G.; Ni, J. *J. Magn. Magn. Mater.* **2008,** 320, 1921.
42. Jacobo, S. E.; Aphesteguy, J. C.; Anton, R. L.; Schegoleva, N. N.; Kurlyandskaya, G. V. *Eur. Polym. J.* **2007,** *43*, 1333.
43. Reddy, K. R.; Lee, K. P.; Gopalan, A. I. *Colloid Surf. A* **2008,** *320*, 49.
44. Yang, H. Y.; Jiang, W.; Lu, Y. *Mater. Lett.* **2007,** *61*, 2789.
45. Koenig, S. H.; Kellar, K. E. *Magn. Reson. Med.* **1995,** *34*, 227.
46. Roch, A.; Muller, R. N.; Gillis, P. *J. Chem. Phys.* **1999,** *110*, 5403.
47. Bulte, J. W. M.; Brooks, R. A.; Moskowitz, B. M.; Bryant, L. H.; Frank, J. A. *Magn. Reson. Med.* **1999,** *42*, 379.
48. Kellar, K. E.; Fujii, D. K.; Gunther, W. H. H.; Briley-Saebo, K.; Bjornerud, A.; Spiller, M.; Koenig, S. H. *J. Magn. Reson. Imaging* **2000,** *11*, 488.
49. Bulte, J. W. M.; Vymazal, J.; Brooks, R. A.; Pierpaoli, C.; Frank, J. A. J. *Magn. Reson. Imaging* **1993,** *3*, 641.